Recent System Test Results from the CMS Tracker Outer Barrel (TOB) Detector.

Juan A. Valls

CERN, 1211 Geneva 23, Switzerland
valls@cern.ch

Abstract

The CMS inner tracking strategy relies on the SST (Silicon Strip Tracker) detector. The six outermost central layers of the SST form the TOB (Tracker Outer Barrel) detector which includes about 5000 individual silicon detector modules. The TOB silicon modules, the services and cables, and the electronics needed for the functioning of the detectors are installed into independent supporting readout elements called RODs. In this paper we report on the results from recent system tests performed at CERN to validate the design and operation of prototype RODs assembled with final components. The main measurements covered here include the electrical performance of individual modules and its comparison with the ROD multi-module setup, the optimization of the working point of the electronics on RODs, optical link verification studies, the characterization of the system in terms of noise and signal to noise ratios, the validation of the shielding and grounding scheme, thermal behavior studies and cooling performance of RODs.

I. INTRODUCTION

The RODs are compact units, easy to handle and mechanically robust, where the TOB silicon detector modules and the services can be tested in stand-alone mode for all their functionality. The main load carrying elements of the ROD are carbon fiber C-profiles interconnected with carbon fiber cross-links that guarantee the integrity of the structure. The services are arranged along straight paths inside the RODs, or on top of the modules, to minimize the assembly work, costs, and failure risk. One of the ROD ends serves as a miniature patch panel where all cables and service lines end. Optical fibers are joined via MT connectors at the end of the ROD. The gas inlet and outlet pipes are realized in stainless steel and run along the two C-profiles of the ROD. They are tied, through an aluminum heat removal plate, to the top surface of each module positioning insert. Figure 1 shows a fully assembled ROD without detector modules inserted.

Two full RODs with final electrical and mechanical components have been assembled and fully excercised at the TOB system test setup at CERN during 2002 and 2003. One ROD includes 6 modules (single-sided SS ROD) and the other includes 12 modules arranged in a double sided back to back configuration (double-sided DS ROD). Both of them include optical readout fibers and electrical trigger and controls links.
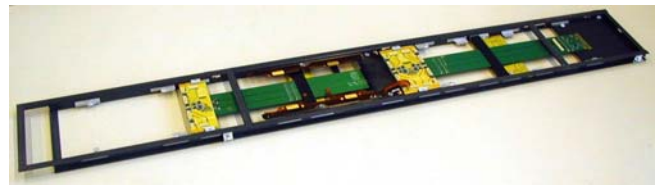
Figure 1: View of a ROD without silicon modules.

The system tests measurements have provided a way to validate the electrical and mechanical design of RODs, optimize the integration of its components and fine tune design details. The main focus of the system tests has been to verify the overall system performance of RODs as compared to its component module characterization, verify the analogue and control readout chains, the signal integrity (distribution of fast control signals like clocks and resets), power distribution (voltage drops and uniformity of supply voltage distribution), and the mechanics and cooling thermal behavior.

The analogue readout chain of RODs has been studied by optimizing the optical link gain and bias points of optohybrids populating the RODs, the time alignment of modules, the identification of noise contributions, crosstalk and common mode noise effects, and operation margin widths. The control chain has been studied by the understanding of the grounding, cabling and shielding schemes as well as operation margin widths.

Results of the TOB silicon detector modules mounted on the first assembled RODs are given in terms of noise, noise occupancies, signal to noise ratios and signal efficiencies. The noise figures from the multi-module ROD setup (optical readout) are compared to the OTRI single module setup (electrical readout). Both test setups show a small or negligible common mode noise picked up by the modules. Similar noise results are obtained in both setups after full calibration gain values are applied. We measure total noise values of ~1600 electrons in peak mode and ~2600 electrons in deconvolution mode. Signal to noise ratios have been studied from beta source and cosmic ray data and are found to be of the order of 15 (25) for deconvolution (peak) operation modes.

The noise occupancies on the modules have important implications on the zero suppression algorithms which the CMS Tracker FEDs (Front End Drivers) will use to reduce the data volume flowing to the DAQ. Here the detector signal efficiencies and noise occupancies are also shown as a function of threshold for a particular clustering algorithm. Signal efficiencies versus noise occupancy plots could also be used to grade detector modules in RODs during production

During production, the assembly of the different electrical components of the RODs (main interconnect bus, interconnect cards and CCUM modules) is done at the industry. The final integration, electrical qualification, and functionality tests of RODs will be done at CERN and collaborating institutes [1]. Most of the results and tools developed during the system test validation phase will be used also during production. The production of the ~760 RODs which form the TOB detector is starting by the fall of 2003.

II. SYSTEM TEST SETUP

The prototype RODs were equipped with 6 (SS ROD) and 12 (DS ROD) TOB modules assembled at FNAL with Doracil ceramic hybrids. Each detector module is optically readout through Analog OptoHybrids (AOH) and optical fibers. Each AOH contains 2 or 3 laser drivers, each with pulse height information from pairs of 128 channels front-end chips (APVs). The light from the optical fibers is converted into electrical signals through a VME based analog to optical converter board. The data is finally digitized in PMC-FEDs. The noise performance of the modules in the optical ROD is compared to the single module test system, based on an OTRI setup with a full electrical readout.

All data has been taken with a DAQ setup based on the TSC (Trigger Sequencer Card), a PMC-FEC (Front-End Control) card with electrical controls and 3 PMC-FED cards using the XROD DAQ program [2]. Special pedestal runs with internal triggers at fixed rates and a random trigger pipeline were taken for the noise studies. Signal to noise measurements and signal efficiencies were also performed from a Ru[106] radioactive source and cosmic ray data runs taken with scintillators connected to NIM logic electronics. The scintillator signal is forced to come within a time window in the corresponding 25 ns integration cycle. During data taking, all modules in the ROD were kept at a full depletion bias voltage of 200 Volts. All results shown in the next sections correspond to both peak and deconvolution APV operation settings.

III. RESULTS

A. Control Timing Characterization

After ROD assembly the first measurement performed was the synchronyzation of the whole system to ensure all front-end APVs sample signals at the same time.
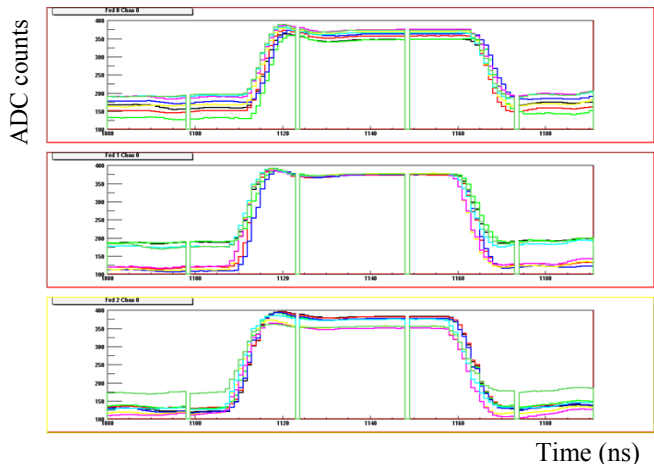
Figure 2: Distribution of PLL scans for the 24 optical links from the DS ROD arriving at the FEDs. Each plot corresponds to a single FED (8 channels).
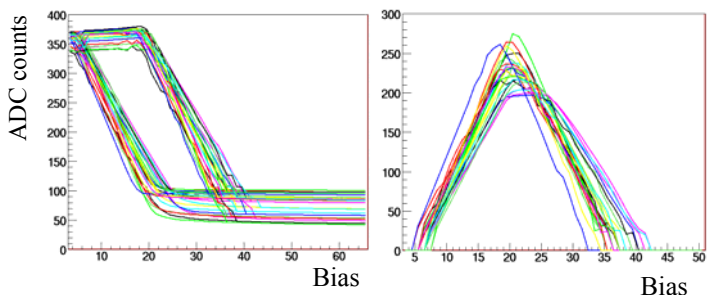
Figure 3: Tick mark and baseline distributions as a function of bias (left) and tick mark amplitudes as a function of bias (right) for the 24 optical FED inputs. All results correspond to a gain G=1.

Control and trigger signals are sent to both the FEDs and the front-end electronics through the FEC. We use the APV synchronization pulses (tick marks) to extract relative timing offsets between the APV chips by triggering the FED in "scope" mode. These delays characterize the position of the APVs inside the RODs and can be adjusted through PLL chips in the front-end. Figure 2 shows a PLL scan distribution for the 8 channels of each of the 3 FEDs used to readout the DS ROD. The relative PLL delay lengths to time align the system is of the order of ~2 ns. Optimal digitization points at the FED level were also obtained for each of the FED channels.

B. Optical Characterization

In order to operate with optimal settings the AOHs, we performed an optical scan characterization of the bias and gain settings for each of the laser drivers of the AOHs. This will be part of the functionality tests to be performed during assembly and later during integration of the detector. The optical characterization scan starts by digitizing the APV tick marks and baselines running the FEDs in "scope" mode as described in last section. The tick marks distributions are then compared with APV baselines for different bias and gain settings of the laser drivers.
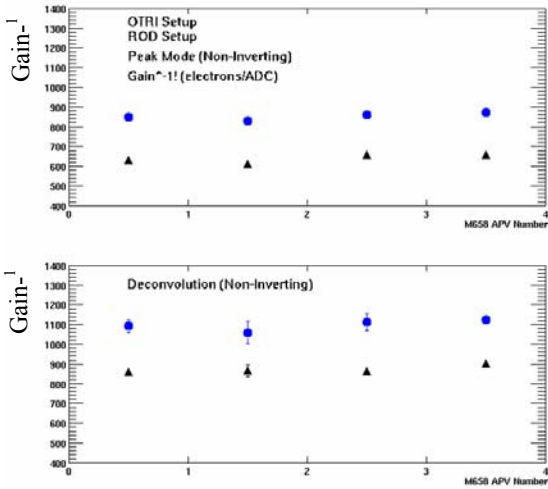
Figure 4: Average gain^{-1} per APV (in electrons/ADC count) for a particular module. There are 4 APVs per module. Results are given for a ROD setup (triangles) and the single module OTRI setup (circles) for peak (top) and deconvolution (bottom) modes.

Figure 3 shows the APV tick marks, baselines, and the tick amplitudes as a function of bias for a gain G=1 and for the 24 optical readout fibers of the DS ROD. The optimal bias and gain operation points for each optical fiber is obtained by comparing the tick amplitude distributions for each gain and bias with the expected FED response to an input signal amplitude of 800 mV.

C. Noise Studies

All noise results are given in terms of the total raw noise (RMS of the pedestal distribution), the common mode substracted noise (CMN), and the differential noise defined as $1/\sqrt{2}$ of the standard deviation of the difference between the output voltage of adjacent strips [3]. A comparison of the total and differential noise for a particular module placed in the ROD setup (optical readout) and in the single module setup (electrical readout) show noise figures in the ROD ~30% larger than in the OTRI setup. Full gain scans in both setups (optical ROD and electrical OTRI) were performed in order to calibrate the systems. Figure 4 shows the full gain results for the ROD and OTRI setups. Gain results are given in electrons per ADC count (where we assume the APV register Ical = 29 correspond to ~ 25000 electrons). The fit gain range spans the linear region of the output signal amplitude (between ~1 and ~3 MIPs). For peak mode with the inverters switched off, the fit gain results yield ~850 electrons/ADC for the OTRI setup and ~650 electrons/ADC for the ROD setup. In deconvolution mode the fit gain yields ~1100 electrons/ADC for the OTRI setup and ~850 electrons/ADC for the ROD setup. From these results the noise figures result in ~1600 electrons in peak mode and ~2600 in deconvolution mode for the ROD setup. Similar results are obtained for OTRI setup (see Figure 5).
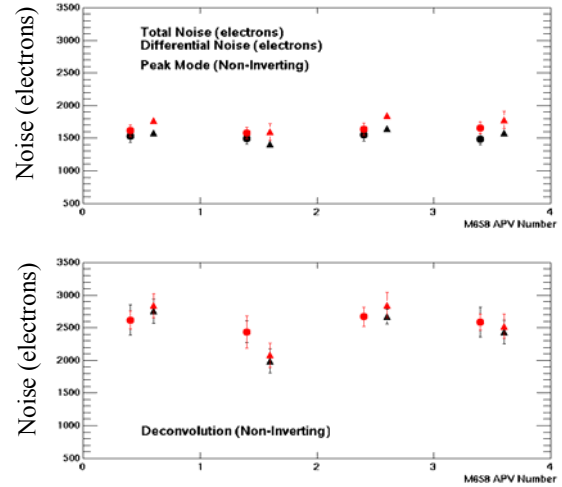
Figure 5: Total and differential noise (in electrons) averaged per APV for a module placed on the ROD (triangules) and in the single module OTRI setup (points). Note the four APVs per module. Top plot is for peak mode and bottom for deconvolution mode.
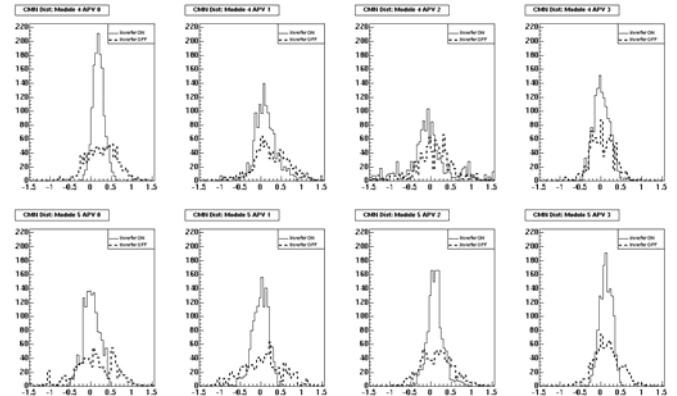
Figure 6: CMN distributions per APV for modules 4 (top) and 5 (bottom). All results for shown for deconvolution mode with inverters on (solid histograms) and off (dashed histograms).

Both the multi-module ROD setp and the single module OTRI setup show a negligible common mode noise (CMN) picked-up by the modules. This indicates a good grounding design of the modules and DAQ electronics. Figure 6 shows the distribution of the CMN per APV for two modules placed in the DS ROD. Results are shown in deconvolution mode with APV inverters on and off.

D. Thermal Behavior

The cooling performance of both ROD prototypes has been verified by measuring the temperature of various parts of the RODs with thermistors and external probes for different ambient and coolant temperatures.
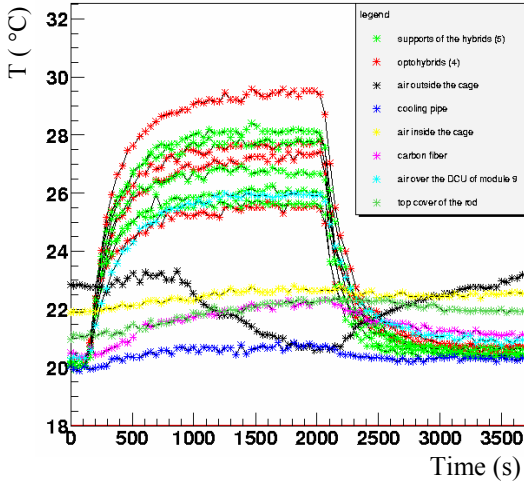
Figure 7: Temperature (in °C) of the different ROD components as a function of time (in seconds) for a thermal cycle off-on-off.

Figure 7 shows the temperature of various ROD parts as a function of time for a thermal cycle with power off-on-off. The relative difference of the different components with respect to the pipe is always below the design 10° C.

E. Signal to Noise Ratios

We have analyzed data taken from a Ru[106] beta source placed directly on top of two back-to-back modules of the ROD. Special runs were also taken with cosmic rays. The algorithm used for cluster finding is based in the following criteria [3]:

- Cluster candidates are formed by selecting strips in a silicon detector module with a signal to noise ratio S/N>5 ("seed" strips).
- Adjacent strips to the "seed" strip are then added to the cluster only if their S/N>2.

The signal of a cluster is the sum of the signals of its strips. This definition is generally more susceptible to systematics coming from the geometrical setup (trigger scintillator configuration), multiple scattering issues and path length from tracks, angle of incidence of particles in the silicon, etc. We will thus show the results in terms of the charge of the "seed" strip. The noise of the cluster is defined as the noise of the "seed" strip. Although the S/N>5 cut does not eliminate signal it is still insufficient to remove all noise clusters. By setting high thresholds one risks to remove clusters with low charge and bias the measured charged distribution yielding artificially high signal values. The thresholds to be used should minimize the number of clusters coming from noise fluctuations without sculpting the signal. The final clustering threshold to be applied in the analysis is thus obtained by finding the lowest thresholds were noise clusters are not significant while not sculpting the signal.

Both signal and S/N distributions are fit to a Gaussian noise function convoluted with a Landau distribution.
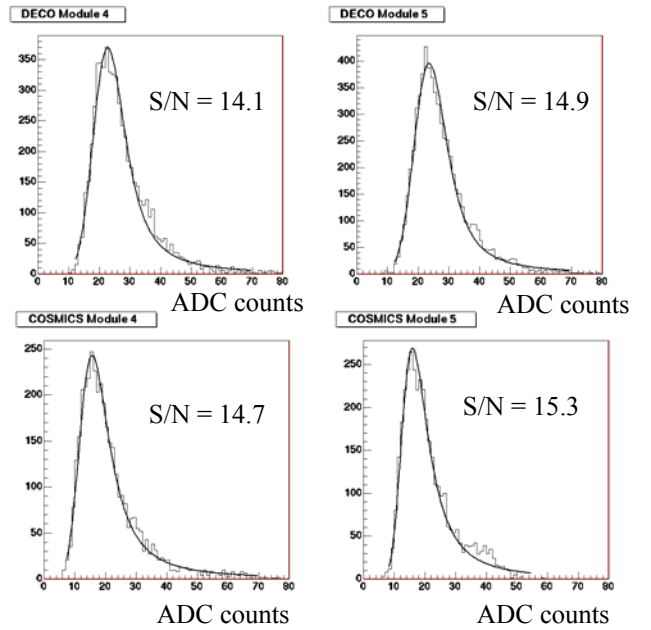
Figure 8: S/N distributions (in ADC counts) for two different modules in the DS ROD (modules 4 and 5 in the plots). The top plots show the results from the beta source. The bottom plots correspond to cosmic ray data. All results correspond to deconvolution mode.

Signal to noise ratios greater than 10 are required along the silicon detector lifetimes for MIPs to ensure signal efficiencies close to 100%. The S/N results when the signal charge distribution is calculated as the "seed" strip signal accounts to ~15 (25) in deconvolution (peak) mode from both the beta source and the
cosmic data (see Figure 8). These results are in agreement with past test beam data.

F. Noise Occupancies and Signal Efficiencies

One of the functionalities of the CMS tracker final FED modules (Front-End Drivers) is the possibility to run a cluster finding algorithm (zero-suppression) applied during data taking. This will reduce the output data rates sent to the DAQ as only strips associated with clusters will be readout. In order for a LVL1 100 kHz trigger rate to remain possible, the mean strip occupancy in the tracker should be less than 1.8% [4]. There will be thus a threshold value to be applied for a particular cluster algorithm which reduces the noise occupancy below this value.

We have studied the signal efficiencies and noise occupancies of individual detector modules as a function of threshold. A cluster finding algorithm based on S/N thresholds as the one described in Reference [4] and Section E is used here. Signal efficiencies are calculated using data taken with a Ru[106] beta radioactive source and cosmic ray data. Noise occupancies are calculated from pedestal runs. Figure 9 shows the signal efficiency as a function of noise occupancy for different thresholds. Results are shown for two particular modules placed in the DS ROD and from cosmic ray data taken in deconvolution mode.
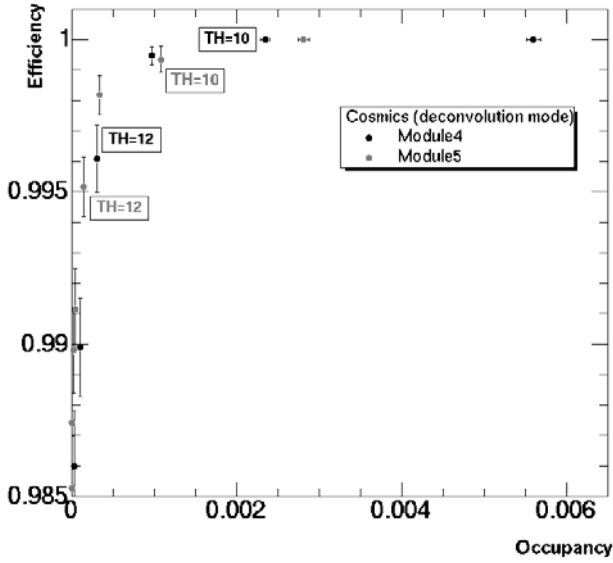
Figure 9: Signal efficiency as a function of noise occupancy for different threshold values (in ADC counts) and two different modules in the DS ROD.

IV. CONCLUSIONS

We have characterized the performance of the two first assembled prototype RODs with final components in a system test setup at CERN. The ROD mechanical and electrical design has been validated with optical readout and electrical controls. The grounding scheme has also been found satisfactory. The cooling performance and thermal bahavior has also been studied and verified at room temperature. The noise performance and signal to noise ratios have been measured and signal efficiencies as a function of noise strip occupancies calculated for different thresholds. In general the overall performance of RODs is validated and the project is ready for production of the ~760 RODs which from the TOB detector.

V. REFERENCES

[1] Assembly and Characterization of Cabled RODs During Production at CERN, F. Ahmed, G. Magazzu, J. Valls, CMS Internal Note CMS IN 2003-025. See also: http://cern.ch/valls/CMS_SST/rod_production.html.

[2] XROD – A Program for ROD Characterization and ROD System Tests, Juan Valls, CMS Internal Note CMS IN 2003-026. See also: http://cern.ch/valls/CMS_SST/xrod.htm.

[3] Performance of CMS TOB Silicon Detector Modules on a Double Sided Prototype ROD, Joaquin Poveda and Juan Valls, CMS Note submitted for publication. See also: http://cern.ch/valls.

[4] On Calibration, Zero Suppression Algorithms and Data Format for the Silicon Strip Tracker FEDs. I. R. Tomalin, CMS-IN 2001/25.

Signal efficiency versus noise occupancy plots could also be used to estimate the efficiencies associated to particular thresholds and define, in this way, figures of merit for grading detectors in RODs based on signal efficiency values.

Table 1 shows the signal efficiencies calculated for two different modules and for different noise occupancy values (corresponding to different σ noise cut levels).

Table 1: Signal efficiency values (in %) associated to different noise occupancy levels for two modules in the DS ROD. Results are shown for both beta source and cosmic ray data.

	Occupancies	Source (peak mode)	Source (deconv. mode)	Cosmics (deconv. mode)
MODULE 4	1 σ (15.9 %)	100 %	100 %	100 %
	2 σ (2.3 %)	100 %	100 %	100 %
	3 σ (0.14 %)	(98.0 ± 0.3) %	(99.7 ± 0.1) %	(99.9 ± 0.1) %
	4 σ (0.003 %)	(94.5 ± 0.3) %	(96.4 ± 0.2) %	(98.6 ± 0.2) %
	5 σ (0.00003 %)	(93.4 ± 0.4) %	(94.8 ± 0.2) %	(97.3 ± 0.3) %
MODULE 5	1 σ (15.9 %)	100 %	100 %	100 %
	2 σ (2.3 %)	100 %	100%	100%
	3 σ (0.14 %)	(99.1 ± 0.3) %	(99.9 ± 0.1) %	(99.9 ± 0.1) %
	4 σ (0.003 %)	(97.6 ± 0.2) %	(99.2 ± 0.2) %	(99.1 ± 0.2) %
	5 σ (0.00003 %)	(94.6 ± 0.4) %	(98.8 ± 0.2) %	(98.8 ± 0.2) %